



Poisoning of SCR Catalysts used in Municipal Waste Incineration Applications

Jan G. M. Brandin¹ · C. U. Ingemar Odenbrand²

Published online: 5 July 2017

© The Author(s) 2017. This article is an open access publication

Abstract A commercial vanadia, tungsta on titania SCR catalyst was poisoned in a side stream in a waste incineration plant. The effect of especially alkali metal poisoning was observed resulting in a decreased activity at long times of exposure. The deactivation after 2311 h was 36% while the decrease in surface area was only 7.6%. Thus the major cause for deactivation was a chemical blocking of acidic sites by alkali metals. The activation–deactivation model showed excellent agreement with experimental data. The model suggests that the original adsorption sites, from the preparation of the catalyst, are rapidly deactivated but are replaced by a new population of adsorption sites due to activation of the catalyst surface by sulphur compounds (SO_2 , SO_3) in the flue gas.

Keywords Poisoning · Waste incineration · SCR catalyst · Modelling of activation and deactivation

1 Introduction

The Selective Catalytic Reduction (SCR) technique, for reduction of NO_x with ammonia, was originally invented in the early 60s, developed in Japan in the 70s and introduced in Europe in the 80s. From the beginning, the technique was used in large stationary boilers and nitric acid plants. Today the concept has developed further and comprises

mobile applications like marine and automotive diesel engines.

During this period, from the 60s till today, a significant change in the feedstock for the stationary boilers has occurred. Due to the concern about greenhouse gases, the use of renewable fuel has increased, in order to reduce the use of fossil fuel. Renewable fuel can be, for instance, woody biomass and forest residues, municipal, industrial or agricultural waste.

While the previous use of fossil gas, diesel or oil produced a rather particulate free flue gas, the new fuels contain larger amounts of alkali metals. Thus, they generate a large portion of fly ash. A recent study compares the use of SCR to SNCR for reduction of nitrogen oxides [1]. The authors say that if the NO_x level for waste incinerators would be lowered to 100 mg/Nm^3 , it will become necessary to use SCR instead of SNCR. For new installations, the catalyst should be placed after the boiler in a high dust position. This means that fly ash will pass through the catalyst bed via the monoliths channels, resulting in a close contact between the catalyst and the fly ash. There are many potentially poisonous compounds in the fly ash. Among them alkali metals are of a major concern [2–5]. They cause deactivation of the catalysts, by blocking the Brønsted acid sites, in the same way as for applications burning forest residues [2, 6].

We have studied SCR catalysts in various applications since the mid 80ies [7, 8]. In one paper, we published the effect of lead on the activity [9]. Earlier results from deactivation studies on diesel engine driven power plants in Sweden [10] show that there is an activation after about 900 h on stream. In that case, the conversion increased from 85 to 92% at 350°C . In an earlier study we showed [11] that gas phase sulphating by 500 ppm SO_2 in 500 ppm NO , 4% O_2 and 4–5% H_2O with He as

✉ Jan G. M. Brandin
Jan.Brandin@LNU.se

¹ Department of Built Environment and Energy Technology, Linnaeus University, 351 46 Växjö, Sweden

² Department of Chemical Engineering, Lund University, P.O. Box 124, 221 99 Lund, Sweden

carrier gas at 400 °C for 21 h created new acidic sites on the catalyst thereby increasing its activity.

The aim of this study is to clarify the reason for the activity as a function of time on stream when using SCR in a waste incineration plant. We show how K and Na in the fly ash deactivate a commercial V_2O_5/WO_3-TiO_2 catalyst. The fly ash and its thermal stability is studied separately in order to explain the results from the poisoned catalysts. A model is described, which correlates the activity of the poisoned catalyst to the time on stream.

2 Experimental

2.1 Deactivation Procedure

The catalyst was a commercial V_2O_5/WO_3-TiO_2 strengthened by silica fibres. Its supplier cannot be stated because of agreement reasons. From the large monolith four 200 mm long, 150 × 150 mm monoliths with wall thickness of 1.1 mm and channel side 6.4 mm were used. They were placed in a deactivation chamber in a side stream of the main flue gas channel (Fig. 1). The gas flow was from top to bottom. Due to limitations at the incineration plant, the slipstream had to be taken after the catalytic bed. This decreased the dust load in the deactivation chamber. However, one can expect that it is mostly large and heavy particles that are separated from the flue gas. The small ones remain and they are prone to catalyst deactivation.

The monoliths were subjected to the conditions below for various lengths of time. After the first monolith was

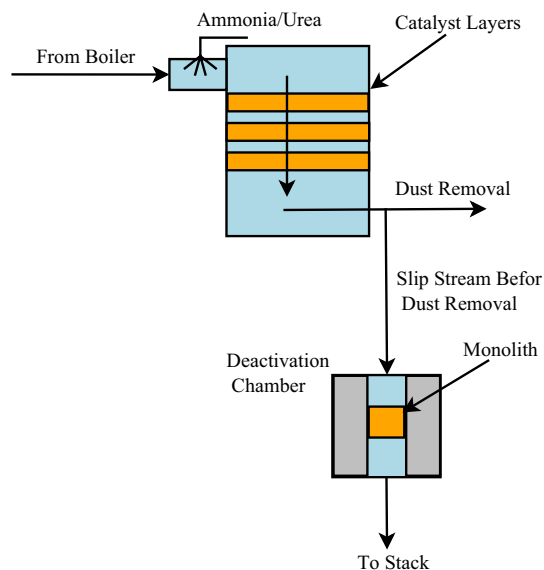


Fig. 1 Slip stream setup at the waste incineration plant

removed, a new one was inserted in its place for further deactivation. In all seven deactivated and one fresh monoliths were analysed.

The condition in the deactivation chamber were; temperature 230 °C, NO_x 60 and NH_3 20 mg/Nm³, O_2 2%, SO_2 350 vppm and space velocity 5000 h⁻¹.

2.2 Measurement of Catalyst Activity

The activities of fresh and deactivated catalyst samples were determined with the same equipment as used before [9]. Samples (one channel 6 cm long) were cut from the larger monoliths from the inlet and the outlet sections as shown in Fig. 2. Most of the data used in this paper were taken from the inlet section.

Based on earlier experience, one can expect a time dependent gradient of catalyst poisons, mainly Na and K, along the length of the monolith. However, in this paper we mostly deal with the 60 mm piece from the inlet section of the monolith. It seems to be a reasonable assumption to consider this piece as uniform.

A Balzer QMG 311 mass spectrometer was used for gas analysis. The temperatures at which the activity was measured were from 260 to 400 °C at 20 °C intervals. 40 min' equilibration time was used at each temperature. The gas stream contained 600 ppm NO, 700 ppm NH_3 , and 2% O_2 , with He as the carrier gas containing about 3000 ppm Ar used as an internal standard in the analysis. The flow rate was 900 Ncm³/min, the space velocity was 12,800 h⁻¹, and the pressure was kept at 1.25 bar. The analysis setup is shown in Fig. 3.

The activity is presented as a first order rate constant determined from the following equations:

$$r = -k \times C_{NO} (\text{mol}/\text{cm}^3, \text{min})$$

$$x = ([NO]_{in} - [NO]_{out})/[NO]_{in} = \text{conversion of NO}$$

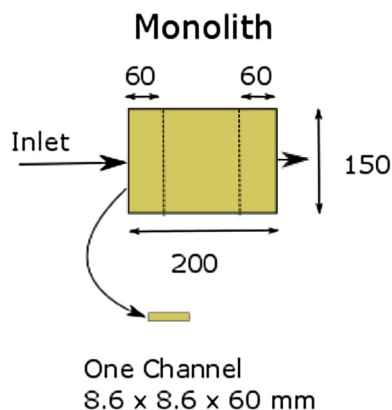


Fig. 2 Samples were taken from the inlet and outlet of each monolith block

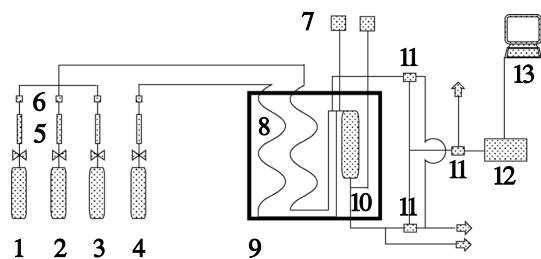


Fig. 3 Experimental setup for determining the catalyst activity. 1, 2, 3, 4 gas cylinders for He, O₂, NO and NH₃, 5 rotameters, 6 flow regulators, 7 pressure sensors, 8 preheating quartz glass tubes, 9 oven with temperature regulator, 10 reactor of quartz glass, 11 3-way valves for choosing gas to analyser, 12 mass spectrometer, 13 computer

$$k = F_0 / ([\text{NO}]_{\text{in}} \times V_{\text{cat}}) \times \ln(1 - x)$$

(first order rate constant based on the
volume of the walls of the monolith, 1/min)

$$k = k_0 \times \exp(-E_a / (R \times T)) \text{ (Arrhenius correlation)}$$

where [NO]_{in} = Concentration of NO in inlet to reactor (mol/cm³); [NO]_{out} = Concentration of NO in outlet from reactor (mol/cm³); k₀ = pre exponential factor (1/min); E_a = activation energy (J/mol); R = gas constant (J/mol/K); T = temperature (K); V_{cat} = catalyst wall volume of the monolith (cm³); F₀ = molar flow of NO into the reactor (mol/min)

2.3 Modelling of the Catalyst Activation/Deactivation

From the activity measurements and the calculated first order rate constants it is obvious that a maximum in activity appears as function of time on stream (Fig. 9). An increased activity has in earlier works [10–12] been attributed to activation of the SCR catalyst by SO₂ in the flue gas. The SO₂ is most likely oxidised by the oxygen present over the V₂O₅ catalyst. The water converts the formed SO₃ to H₂SO₄ and new acidic sulphate groups are formed on the catalyst. On the surface, there are active sites for the SCR reaction (V₂O₅). However, there are also adsorption sites for ammonia. Those adsorption sites are not necessarily active in the reaction, but serve as storage sites for the ammonia on the surface. This means that a decrease of the number of acidic adsorption sites, for instance by alkali poisoning, decreases the reaction rate and an increase of the number of sites, for instance by activation, increases the rate of reaction. This is due to the change in the surface concentration of ammonia.

On the fresh catalyst, there is a population of adsorption sites, formed during the preparation that can be regarded as the original one. Besides this population, there must be a population of proto-sites (N) that can be activated. The

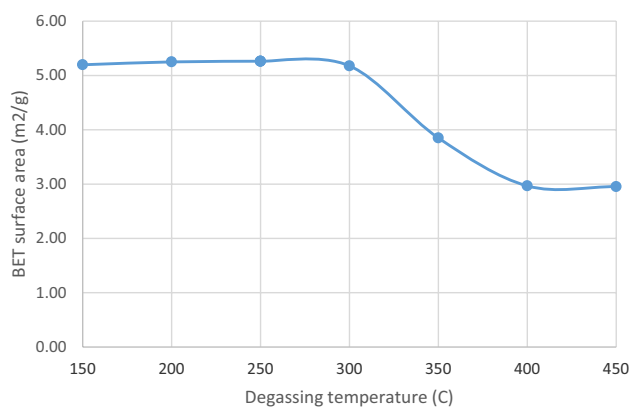


Fig. 4 The BET surface area of the fly ash as a function of degassing temperature

original population of adsorption sites (S1) starts to deactivate as soon the catalyst comes on stream, forming deactivated sites (D1). However as soon the catalyst comes on stream, the proto-sites starts to form active sites (S2). After the formation of the new sites (S2) they in turn start to deactivate (D2). The following model is formulated, at constant temperature, with the deactivation/activation constants c1, c2 and c3:



From these reactions (1 & 2) the following differential equations are set up:

$$\frac{dS1}{dt} = -c1 \times [S1] \quad (3)$$

$$\frac{dS2}{dt} = c2 \times [N] - c3 \times [S2] \quad (4)$$

A balance over the proto-sites gives:

$$[N0] = [N] + [S2] + [D2] \quad (5)$$

Eliminating N in (4) by the use of (5) gives:

$$\frac{dS2}{dt} = -c2 \times ([N0] - [S2] - [D2]) - c3 \times [S2] \quad (6)$$

D2 can't be eliminated, so one further differential equation is needed:

$$\frac{dD2}{dt} = c3 \times [S2] \quad (7)$$

This model describes the time dependent populations of adsorption sites, S1 and S2. Equation (3) have the analytical solution, were S0 is the initial number of sites

$$S1(t) = S0 \times e^{-c1 \times t} \tag{8}$$

The equations 6 & 7 have to be integrated simultaneously.

In this work a pseudo-first order reaction in nitrogen monoxide is considered

$$r_{NO} = -k_1 \times C_{NO}$$

However, the reaction is bi-molecular and normally described with an Eley–Rideal rate expression.

$$r_{NO} = -k_1 C_{NO} \times \theta_{NH3}$$

$$\theta_{NH3} = \frac{k_a \times C_{NH3}}{1 + k_a C_{NH3}}$$

where θ_{NH3} is the coverages of ammonia on the catalyst surface. Now, if ammonia is in excess and $k_a C_{NH3} \gg 1$ the $\theta_{NH3} \Rightarrow 1$ and the rate expression becomes pseudo-first order in NO. This is normally the case below 400 °C.

The θ_{NH3} varies only between 0 and 1 so the information about the number of adsorption sites becomes bundled up in the rate constant k_1 .

$$k_1 = a_0 e^{\frac{-E_a}{RT}}$$

The frequency factor should be proportional to the total number of adsorption sites:

$$a_0 = a'_0 \times S$$

where S is the number of sites.

It is now assumed that there are two parallel pathways for the reaction that are identical, except for the number of adsorption sites for each pathway. Then the observed rate constant (k_{tot}) will be the sum of the two rate constants.

$$\begin{aligned} k_{tot} &= k_1 + k_2 = a_1 \times e^{(-E_a/RT)} + a_2 \times e^{(-E_a/RT)} \\ &= a_0' \times S1 \times e^{(-E_a/RT)} + a_0' \times S2 \times e^{(-E_a/RT)} \\ &= a_0' \times e^{(-E_a/RT)} \times (S1 + S2) \end{aligned}$$

$$\begin{aligned} k_{tot} &= a_0' \times S1_0 \times e^{(-E_a/RT)} \times (S1/S1_0 + S2/S1_0) \\ &= k1_0 \times (S1/S1_0 + S2/S1_0). \end{aligned}$$

where 1 and 2 are the indexes for the first and second reactions, $S1_0$ is the initial number of adsorption sites in the original population and $k1_0$ is the initial, the fresh, rate constant of the catalyst. Initially, at $t=0$, $S1=S1_0$ and $S2=0$ so $k_{tot} = k1_0$.

The model was solved by searching for a symbolic solution in Maple.

The symbolic solution by Maple was:

$$S1(t) = k1(0) \times e^{-C1 \times t}$$

$$S2(t) = \gamma2 \times \frac{C2}{C3} \times e^{-C2 \times t} + \gamma1 \times e^{-C3 \times t}$$

$$D2(t) = \gamma2 \times e^{-C2 \times t} + \gamma1 \times e^{-C3 \times t} + N0$$

where $\gamma1$ and $\gamma2$ are integration constants.

However, at $t=0$ $S2=0$ and $D2=0$

$$\gamma2 = -\gamma1 \times \frac{C3}{C2}$$

$$N0 = -(\gamma1 + \gamma2)$$

The symbolic solution was entered into Excel and calculated in about 50 time steps between 0 and 2500 h. At each step the resulting rate constant $k_{tot} = k1_0 \times (S1 + S2)/S1_0$ was calculated.

Now, the resulting rate constant for the SCR reaction is a function of unknown parameters: the deactivation constants C1 and C3, activation constant C2 and the initial number of proto-sites N0.

The unknown parameters were tuned and the resulting rate constant (k_{tot}) was plotted against the measured rate constant as function of time. A least square sum between the resulting rate constant and the measured constant was set up. When the resulting rate constants were near the measured constants, the built in Excel optimizer (Solver) was used to fine-tune the parameters by minimizing the least square sum.

2.4 Measurement of Catalyst Composition by AAS

About 0.7 g of the catalyst samples (1 cm of the mini monolith from the inlet, Fig. 2) was crushed and finely ground in a mortar. Known weights were dissolved in 25 ml of 40% HF. The solutions were diluted with distilled water to the concentrations needed for analysis. All analyses were done with double or triple samples to lower the influence of analytical errors. The results shown are the mean values of the experimental ones in weight percent. The equipment used was a GSM atomic absorption spectrometer (AAS).

2.5 Analysis by N₂ Adsorption

BET analysis was performed on a piece of the wall of the monolith as well on the fly ash with a Micromeritics ASAP 2400 equipment after outgassing at 0.04 Torr and 90 °C for 1 h and at 400 °C for 24 h to a final pressure of 10⁻³ Torr. Determination of the surface area and the pore size distribution was carried out by physisorption of N₂ at 77 K. The accuracy of the method for measuring the BET surface area is around 1% as determined separately for the experimental conditions used. Samples were also submitted to sintering for up to 144 h at 400 °C to study the stability of the materials. The micro pore volume is calculated by the t-plot method using the t curve from literature [13]. In

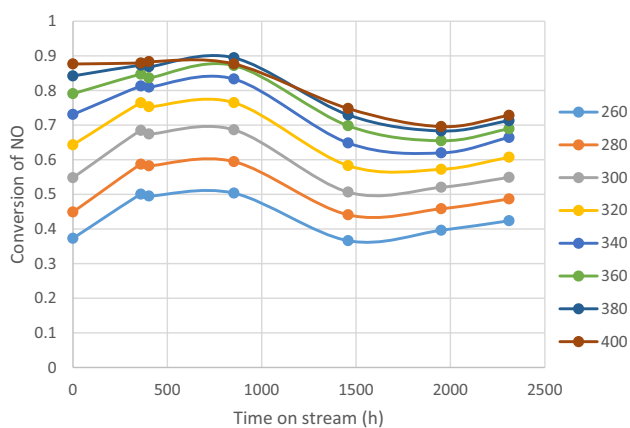


Fig. 5 Experimental conversion of NO as a function of time on stream stream at various temperatures ($^{\circ}\text{C}$) 600 ppm NO, 700 ppm NH_3 , and 2% O_2 , with He as the carrier gas containing about 3000 ppm Ar. Flow 900 Ncm^3/min , space velocity 12,800 h^{-1} , pressure 1.25 bar

Table 1 BET and micro pore surface area degassed various times at 400 $^{\circ}\text{C}$

Time (h)	BET surface area (m^2/g)	Micro pore surface area (m^2/g)
0	63.1	4.3
0.25	65.1	4.4
0.5	64.4	3.6
1	62.5	3.5
2	63.6	4.3
4	62.4	4.9
16	64.6	5.0
32	64.4	5.9
72	62.2	6.4
Mean	63.6	4.7
SD	1.0	0.9

all measurements the degassing temperature was varied in order to see the effect of this parameter.

3 Results

3.1 Surface Area of Fly Ash at Increasing Degassing Temperatures

Different degassing temperatures were used before N_2 adsorption studies. The degassing lasted for 24 h. As seen in Fig. 4 something happens to the ash above 300 $^{\circ}\text{C}$ decreasing the surface area by 42% at 400 $^{\circ}\text{C}$. This decrease is especially noted in the micro pore surface area, which decreases from 1.99 to 0.29 m^2/g from 150 to 450 $^{\circ}\text{C}$. The

decrease in this case is 85%. The micro pore volume also decreases by 86.5% from 0.00089 cm^3/g .

3.2 Stability of the Surface Area of the Fresh Catalyst

There is very little if any effect of the degassing time on the BET surface area of the fresh catalyst up to 72 h as seen in Table 1. The mean value is 63.6 m^2/g with a standard deviation of 1.0 m^2/g . This is close to the accuracy of the method. The variation of the micro pore surface area is larger with a mean of 4.7 m^2/g and a standard deviation of 0.9 m^2/g . There is a trend of increasing micro pore area with time. It increases by 49%.

3.3 Effect of Time on Stream Under Deactivation Conditions

3.3.1 Effect on Accumulation of Catalyst Poisons

In the analysis by AAS, the whole catalyst material is analysed. The fresh catalyst elements analysed were in order of decreasing content (wt%): Ti (49), W (7), Si (5.4), V (0.54), Al (0.53), Ca (0.17), Fe (0.14), K (0.056) and Na (0.026). An analysis by SEM–EDAX [14] of the ash showed that it contained 1.6 atom % P, 2.2% Ti, 2.1% Fe, 3.4% Mg, 5.2% Zn, 4.2% Na, 4.5% K, 11.9% Al, 10.4% S, 11.8% Cl, 14.8% Si and 29.3% Ca. Thus a number of components which are known to deactivate the catalyst are present in the fly ash. This phenomenon will be discussed in a further paper [14].

In Fig. 5 are the experimental conversions and their dependence on the time on stream shown. For all temperatures, there is an increased conversion with time. A maximum is reached where after the conversion drops again. At very long times on stream there is no drop in conversion any more.

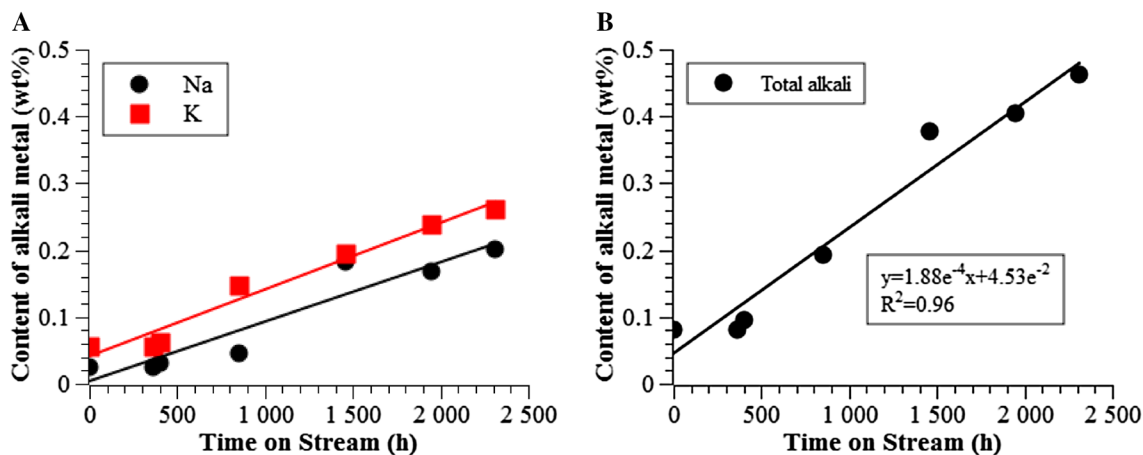
In Fig. 6a, b it is shown that both alkali metal contents increase almost linearly with time.

3.3.2 Effect on Surface Areas (BET and Micro Pore)

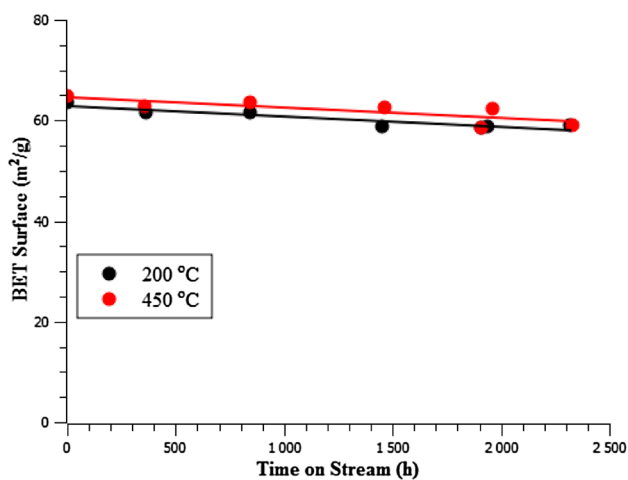
In Fig. 7 the BET surface area as function of time on stream is shown for the lowest and highest degassing temperatures. The BET surface area is decreasing slowly with time on stream. The slopes are very similar, and the statistic evaluation (Appendix) shows that the correlations are significant on the 95% test level. To investigate if there is any difference between the two sets of measurements, a paired comparison was done (Appendix). The results show that the two sets of data differ significantly on the 95% test level. However, since the slopes are identical, the samples differ in the initial surface area only. Since all analysed samples are different specimens, the difference in initial surface area can't be caused by

Table 2 Constants from fitting to the deactivation model at various temperatures

Temperature (°C)	C1	C2	C3	γ_1	γ_{2a}	$N0^a$
340	0.0012	0.0012	0.0011	73.0	-75.8	2.76
360	0.0011	0.0012	0.0008	55.3	-57.4	2.12
380	0.0011	0.0011	0.0011	50.0	-52.2	2.17
400	0.0010	0.0010	0.0011	51.5	-53.1	1.58
Mv	0.0011	0.0011	0.0010	57.5	-59.6	2.16
SD_{mean}	0.000041	0.000048	0.000075	5.3	5.5	0.24
SD_{mean}/Mv	0.037	0.043	0.073	0.092	-0.092	0.112

^aCalculated**Fig. 6** a Effect of time on stream on accumulation of alkali metal catalyst poisons by AAS, b correlation of total alkali content to time on stream

variations in the fresh catalyst. So the small difference in surface area between the two sets of samples (mean value $1.7 \text{ m}^2/\text{g}$) is a result of the increased degassing temperature (from 200 to 450°C). The long term decreases

**Fig. 7** BET Surface areas as function of time on stream for the lowest (200°C) and the highest (450°C) degassing temperature (inlet samples)

in surface areas (average $5 \text{ m}^2/\text{g}$ in 2300 h) is caused by either blocking of pores by non-volatile deposits or by sintering of the catalyst. It amounts to 7.6% of the area of the fresh catalyst.

The micro pore surface area (Fig. 8) decreases rapidly during the 400 h first hours. Then the surface area remains almost constant. The absolute value of decrease in surface area is about twice as large for the BET surface area as for the micro pore area.

3.3.3 Effect on Catalyst Activity

There is an obvious increase in the rate constant after some time on stream (Fig. 9). The maximum is different at different reaction temperatures, around 853 h for 340 to 380°C and 403 h for 400°C reaction temperatures. There seems to be a levelling off of the rate constant at times longer than 1400 h. The activity of the poisoned catalysts is 82, 76, 70 and 64% of the value of the fresh ones from 340 to 400°C at 1951 h. Thus the higher the temperature the more severe is the poisoning effect. The activation, to the point of maximum activity, is 43, 38, 28

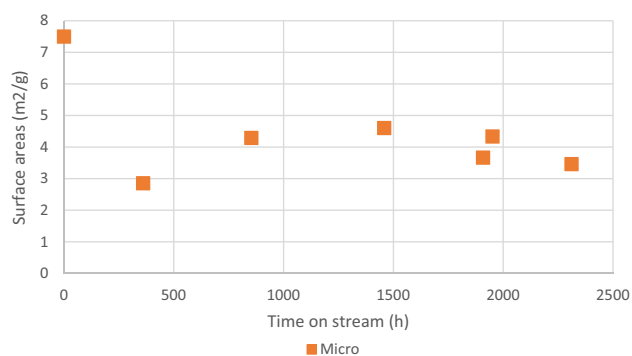


Fig. 8 Effect of time on stream on micro pore surface areas of inlet section of catalyst (degassed for 24 h at 400 °C)

and 13% in the same temperature range. This also shows that the activation is largest at lower temperatures.

The apparent activation energies from the inlet and outlet section (Fig. 10) shows spreading but similar behaviour. To investigate if there was any difference in the two datasets, a paired comparison was done (Appendix). The statistic evaluation shows that the null hypothesis H_0 , no difference between the two data sets, is significant on the 95% level. This can be taken as an indication that the activity does not vary much between the inlet and the outlet.

3.4 Modelling of the Activation–Deactivation Process

The deactivation–activation model described in Sect. 2.3, was fitted to the experimental first order rate constants (Fig. 11). In the fitting, the last point at 2311 h was omitted since it is expected that the rate constant will continue decreasing at further exposure to the flue gas. The reason for deviation might be explained by spreading in experimental data.

In Fig. 11, one can see the fitted model to the calculated first order rate constants from the measured conversions for each catalyst sample. The model describes the activity of the catalyst very well.

Since the rate constant, as function of time on stream, was measured at different temperatures the model was used to fit the constant at all temperatures (Fig. 12).

The fitted constants were the deactivation constants C1 and C3, the activation constant C2 and the integration constant γ from the Maple solution. This means that the initial number of proto-sites N0 and the γ 2 constant are calculated according to Sect. 2.3. The result is presented in Table 2.

We would like to compare our model to earlier studies by Kamata [3]. Thus, Fig. 13 below was constructed from their data.

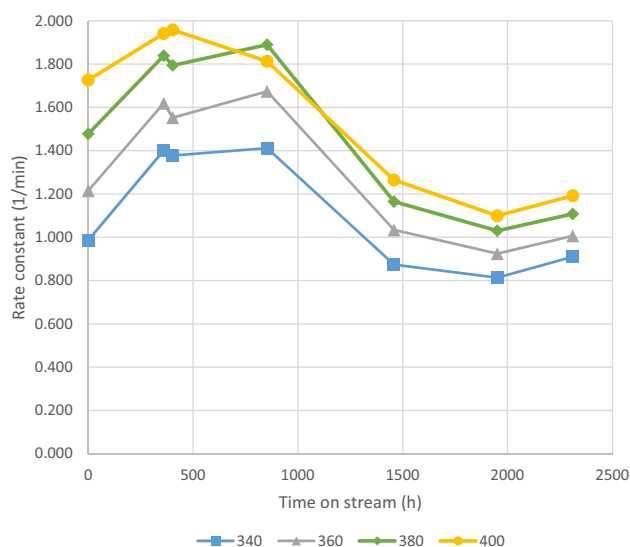


Fig. 9 Effect of time on stream on apparent rate constant for the reduction of NO at four temperatures (340–400 °C) for the inlet part of the monolith

The rate constants, determined at 5 given K contents up to 1wt% were calculated from conversion data. The expression $k = 254.6 \times \exp(-4.8 \times \%K)$ was used to fit their data. The value of the time in our experiment to obtain this amount of K content was estimated by comparing constants normalized to the total rate constant of the model at $t=0$ to the total experimental rate constant. This value of time was used in Fig. 13 to represent the Kamata model.

The model based on the total amount of Na and K uses experimentally determined concentrations (Fig. 6b). To calculate the rate constant, at our experimentally

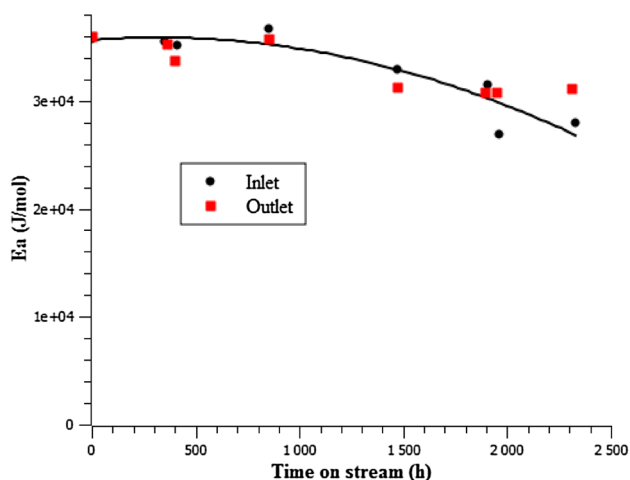


Fig. 10 Comparison of the apparent activation energy as function of time on stream for the inlet and outlet sections

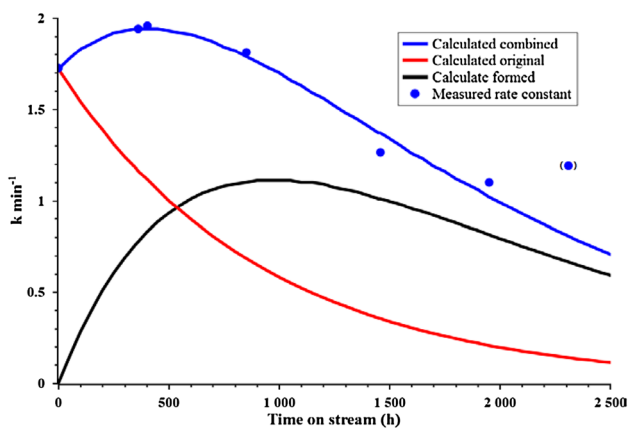


Fig. 11 Fitting of the activation–deactivation model to experimental data, SCR first order rate constant at 400 °C (blue dots). Calculated overall rate constant (blue line), deactivation of initial population of sites (red line), formed secondary sites (black line)

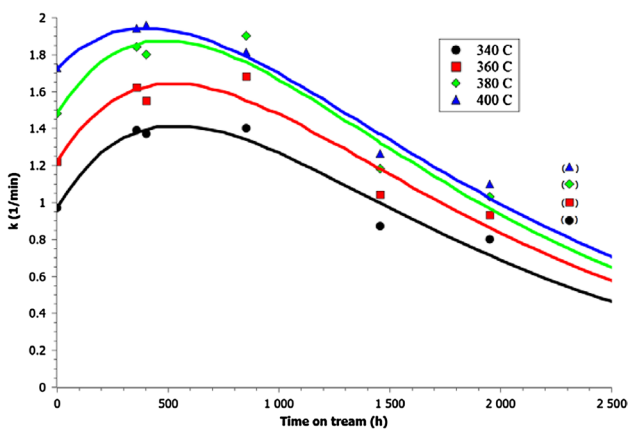


Fig. 12 Fitting of the activation–deactivation model to the different experimental sets of SCR first order rate constants (340, 360, 380 and 400 °C) versus time on stream

determined K contents, for that model the deactivation rate constant versus K% (Fig. 13) was used. These rate constants are normalized as before and plotted in Fig. 14.

The result is that our model predicts a deactivation rate, which is between the two others. The Kamata one shows slower deactivation at longer times while the model based on alkali metal content over predicts the deactivation at short times (Fig. 14).

4 Discussion

It can be noted that the ash contains some components that are melting and blocking the micro pores between 300 and

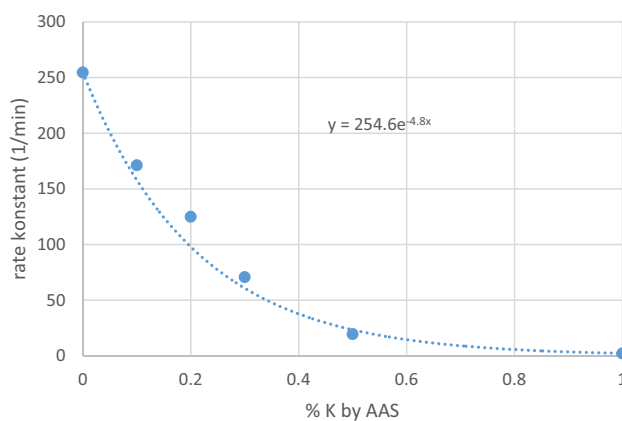


Fig. 13 The rate constant at 400 °C and its dependence on the amount of K constructed from data of Kamata. These catalysts were impregnated with KNO₃

400 °C. One possible candidate is ZnCl₂ with a melting point of 290 °C [15].

The AAS analysis (Fig. 6) is an average of the entire catalyst samples, and the alkali analysis shows close to a linear increase versus time on stream. Earlier studies [2, 3] have shown a strong correlation between the alkali content and the deactivation rate of SCR catalysts. Especially catalyst used in, alkaline rich, highly dusty environments like in biofuel and waste combustion are subjected to strong deactivation. With the measured alkali levels in the SCR catalyst in this study, one would expect a profound effect on the catalyst activity.

After 1951 h on stream the activity, measured at 400 °C, drops by 36% compared to the activity of the fresh catalyst. The surface area drops by only 7%. Thus the major cause for the decreased activity is a chemical effect by blocking of acidic sites by alkali metals.

The initial apparent activation energy (fresh catalyst) is 36 kJ/mol indicates a mass transfer limitation by pore diffusion. The calculated effectiveness factor is 0.52 at 673 K and there is no external limitations for mass or temperature as calculated by methods given by Mears [16–18]. The intrinsic 1st order rate constant is 0.0254 m³/kg_{cat}·s. The main other gradient is along the axis of the reactor. A temperature increase of 4.5 K is calculated. The activation energy decreases non-linearly by time on stream (Fig. 10) both for the inlet and outlet pieces of the monolith. A paired comparison on a 95% confidence level shows that there is no significant difference between the inlet and outlet activation energies (Appendix). The decrease in activation energy could be the result of deactivation of the catalyst from the outer surface towards the centre of the catalyst. This means that the reactants must diffuse through a, with

time increasing, layer of inert material. This increases the mass transport resistance, decreasing the activation energy.

This increases the mass transport resistance resulting in a decreased activation energy. Castellino et al. [3] also show the decrease in activation energy on K₃PO₄ deactivated catalysts from 66 kJ/mol for a fresh catalyst via 49–36 kJ/mol for the most deactivated one. Similar result with apparent E_a of 46 kJ/mol for a fresh and 30 kJ/mol for a 1% V₂O₅-9% W/TiO₂ doped with 0.5 K per V were presented by Baxter [19]. Our most deactivated catalyst, used for 1951 h, has a similar effectiveness factor of 0.66 as the fresh one and is thus only limited by pore diffusion.

However, the initial effect in this study is an increase of activity. The calculated first order rate constants show an increase versus time on stream, at 400 °C the increase is 13% compared with the fresh catalyst. This kind of on stream activation of vanadia based SCR catalyst is known from industrial applications, for instance in the Visby CHP plant and also from our other studies [11], and can be attributed to the sulphur content of the fuel [12, 20]. Vanadia is a well-known oxidation catalyst for SO₂ to SO₃ in the contact production process for sulphuric acid [21]. If the SCR catalyst oxidizes SO₂ to SO₃, a more corrosive flue gas is produced, however an activation of the catalyst occurs at high temperatures (>300 °C) while a deactivation occurs at low temperatures (<250 °C). The deactivation at low temperature is caused by pore plugging due to deposition of ammonium sulphate and ammonium bi-sulphate due to the reaction between SO₃, ammonia and water [22]. This is a limiting factor for low temperature SCR applications and efforts are made to minimize SCR catalysts SO₃ formation [12, 22]. The sulphating of the SCR catalyst, and the formation of acidic sites on stream, is beneficial for the SCR reaction.

According to Dunn [23] the rate of oxidation of sulphur dioxide is very slow compared with the rate of the SCR reaction over supported vanadia catalyst. The TOF for the SCR reaction is 1000–10,000 times higher than that of the SO₂ oxidation at 230 °C. The reason for the low TOF for sulphur oxidation would be the weak adsorption of SO₂ on the vanadium oxide. The formed SO₃(g) desorbs, and re-adsorbs, stronger than SO₂(g), on another vanadium oxide surface site. This inhibits the SO₂ oxidation by competitive adsorption. The formed SO₃(g) could also adsorb on a free TiO₂ surface as suggested by [20]. The adsorbed SO₃, together with water, then forms the new acidic sites, responsible for the activation of the SCR catalyst. If the sulphur dioxide oxidation is so slow, the concentration of SO₂(g) probably is constant through the entire length of the monolith catalyst. This would then mean that the activation of the catalyst occurs over the entire length of the catalyst simultaneous.

There was no sulphur dioxide, neither trioxide, measurements done in this investigation since they were not identified as important prior the measuring campaign. However, the SO₂/SO₃ level that the SCR catalyst is exposed to is about 350 vppm and is much higher than the allowed emission from the plant since the catalytic bed is placed before the Flue Gas De-Sulphurization (FGD) unit.

The calculated activation energies show a non-linear decrease with time for both the inlet and outlet sections (Fig. 10). The paired comparison shows that there is no reason to consider the behaviour of the two sections of the catalyst as different. They are the same, or very similar. The decrease in activation energy might imply an increased diffusion resistance, for instance by poisoning of the catalyst from the outer surface and inwards. This would then result in an increasing diffusion resistance.

The temperature in the deactivation chamber was quit low, 230 °C, and there was a risk that the pore system of the catalyst would be filled up with ammonium sulphate and bi-sulphate. However, the degassing of the catalyst samples at increasing temperatures, from 200 to 450 °C, gave little gain in BET surface area (1.7 m² Fig. 7). The long-term decrease in the BET area is around 7.6% over 2311 h on stream and is the same for samples degassed between 200 and 400 °C. This decrease might be a result of pore clogging with un-volatile material or sintering. However, sintering of the fresh catalyst in the laboratory at 400 °C during 72 h did not cause any significant loss of BET surface (Table 1).

The activation–deactivation model seems to describe the experimental data very well (Figs. 11, 12) except for the last point at 2311 h. One could not see any particular reason why the deactivation should level off or why the catalyst should increase its activity on further exposure, unless something has happened with the gas composition. This could of course happen if the fuel in the combustion; the waste, have changed. There is no information from the incineration plant for such changes, but the campaign lasted for 2300 h so it can't be ruled out. The model suggests that there is a rapid decrease in the original population of acidic sites but this is counteracted by the formation of the new sites. After 500 h the newly formed sites dominate the activity of the catalyst. If this were correct, a rapid deactivation of the catalyst would be the result of exposure to a sulphur free flue gas. The fitting of the model to the data set at different temperatures gives the same activation and deactivation constants, they are not affected by the recording temperature. The deactivation of the catalyst has taken place during the long time exposure in the flue gas, and that is not changed just because the activity of the deactivated catalyst is measured at different temperatures. Looking at the values of NO, they decrease with temperature, which

should be the case for Brønsted acid sites, due to the distribution of heat of adsorption.

In comparing models (Fig. 14), the poisoning effects of K and Na are assumed equal on a wt% basis. This is supported by an investigation performed by Lisi [24]. They also obtained a strong deactivation effect of the alkali metals. Their investigation was also based on impregnated samples, which might give stronger deactivation because of very good penetration of metals to the interior of the catalysts. A very recent study [25] shows the poisoning effects of alkali salts to follow the sequence of $\text{Na}_2\text{CO}_3 < \text{K}_2\text{CO}_3 < \text{Na}_2\text{SO}_4 < \text{K}_2\text{SO}_4 < \text{NaCl} < \text{KCl}$. The salts were introduced during entrained-flow combustion. We have similar conditions and our poisonous components should be the sulphates and the chlorides. Thus our assumption of equal poisoning effects of Na and K led to somewhat too high deactivation rates as shown in Fig. 14 but much better than Kamata’s results based on potassium only.

Alkali rich dusty flue gases, formed for instance in biomass and waste combustion, can give rapid deactivation of the SCR catalysts. It would be very interesting if the S level in the fuel could prolong the catalyst lifetime. In such case, one could try to increase the content in low containing fuels, like pure wood, by mixing with fuels containing higher levels of sulphur, like bark. This could of course lead to other problems in the plant like increased corrosion or increased amount of melting ash.

5 Conclusions

The deactivation of the SCR catalyst is not connected to the loss of BET-surface area; it is a chemical phenomenon. It is clear that Na and K poison the catalyst.

The suggested model describes the activation–deactivation process very well.

It consists of a deactivation of original sites by alkali metals but also a formation of new acidic adsorption sites by interaction with SO_x species in the flue gas. The model seems relevant to evaluate industrially deactivated catalysts. It requires, though, occasional sampling of the catalyst and activity measurement offline.

6 Appendix

Statistical evaluation [26] in Sect. 3.3.2 (Fig. 8).

Two sets of exposed catalysts, between 0 and 2311 h, were degassed at 200 and 400 °C respectively for 24 h. The measured BET surface for each sample in the set was plotted versus the time on stream for the sample. Each

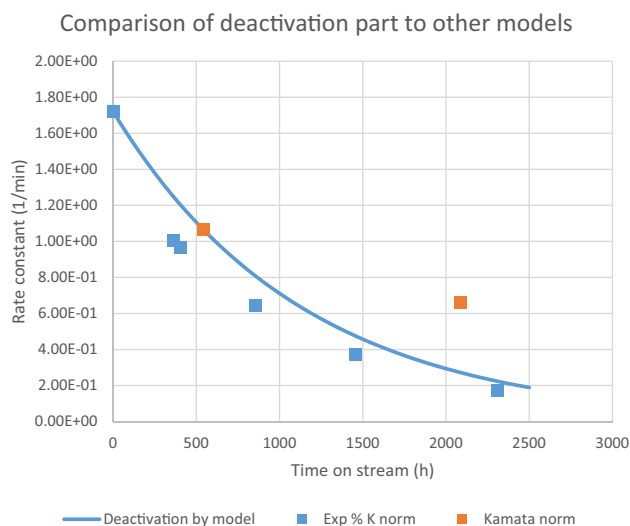


Fig. 14 Comparison of results from the deactivation part of the model to normalized experimental data from Kamata and normalized data calculated from measured Na + K content of the catalysts

data set was then fitted with a straight line by the least square method. The fitted slopes, the 95% confidence intervals and the correlation coefficients (R) are given in Table 3.

To validate the correlation a *t* test was performed.

The null hypothesis, H_0 , is that no correlation exists.

Test quantity $t_{\text{cal}} = R((n-2)/(1-R^2))^{0.5}$.

In the measurement seven points ($n = 7$).

$F = n - 1 = 6$ and confidence level 95%. From the *t*-table $t(f = 6)_{0.95} = 2.45$.

The decreases in BET surfaces are statistically significant at the 95% confidence level. It can be seen from the confidence interval of the slope and from the *t* test of the regression coefficient ($t_{\text{cal}} > t$ -table). This means that the null hypothesis is void.

A paired comparison was done to investigate if the two measurements are identical or can be considered as different, Table 4.

The mean value of the difference is $|X| = 1.67 \text{ m}^2$ and standard deviation $SD_{\text{diff}} = 1.57 \text{ m}^2$.

Null hypothesis: no difference between the data sets

Test quantity $t_{\text{cal}} = (|X| - 0) / SD_{\text{diff}} \times n^{0.5}$.

From the table $t(f = 6)_{0.95} = 2.45$.

$t_{\text{cal}} = 2.89$.

Table 3 Result of the linear least square fitting

Temp (°C)	Slope (m ² /h)	95% CI (m ² /h)	R	$t_{\text{cal}} = R((n-2)/(1-R^2))^{0.5}$	<i>t</i> table
200	-1.89e-3	±0.36e-3	0.92	5.31	2.45
400	-1.63e-3	±0.53e-3	0.80	2.98	2.45

Table 4 Paired comparison of the two sets, degassed at 200 and 400 °C, of BET surface data

Time (h)	0	360	403	853	1458	1951	2311
T 200 °C	63.515	61.6287	61.6707	58.8204	58.4431	58.8623	59.1557
T 450 °C	64.8145	62.7245	63.5711	62.6174	58.517	62.4161	59.1109
Diff	-1.2995	-1.0958	-1.9004	-3.797	-0.0739	-3.5538	0.0448

Table 5 Paired comparison of the activation energies (J/(mol K)) in the inlet and outlet sections

Time h	0	360	403	853	1458	1951	2311
Ea inlet	35,800	35,510	35,212	36,726	32,919	26,858	27,919
Ea outlet	36,000	35,300	33,700	35,700	31,306	30,800	31,200
Diff	-200	210	1512	1026	1613	-3942	-3281

Since the calculated value $2.89 > 2.45$ from table, the null hypothesis is void. The measurements differ. However, since the slopes are the same, the difference lies in the initial surface area, they differ significantly.

Section 3.3.3 Effect on catalyst activity, Fig. 7 One can test two data sets if they are identical or different by a paired comparison. However, the number of samples in each set must be equal. In this case it is the experimentally determined activation energies of the SCR reaction that are compared in the inlet and outlet sections of the monolith (Table 5).

The mean value of the differences X_{diff} is -294.38 J/(mol K) and the SD of the differences is 2143.6 J/(mol K).

Null hypothesis H_0 : no difference between the data sets.

Test quantity $t_{\text{cal}} = (X_{\text{diff}} - 0) / \text{SD} \times n^{0.5}$.

$t_{\text{cal}} = 0.38$.

$f = 7$ and confidence level 95%.

From table $t(f = 7)_{0.95} = 2.37$.

Since $t_{\text{cal}} < t_{\text{table}}$, the null hypothesis is valid. There is no difference between the two data sets.

Acknowledgements We wish to thank Mr Johan Janner who performed the reaction experiments. Mrs Birgitta Lindén helped us with the nitrogen adsorption measurements. A Swedish waste incineration plant is acknowledged for letting us use their facilities for the application of poisons on the catalyst specimen.

Open Access This article is distributed under the terms of the Creative Commons Attribution 4.0 International License (<http://creativecommons.org/licenses/by/4.0/>), which permits unrestricted use, distribution, and reproduction in any medium, provided you give appropriate credit to the original author(s) and the source, provide a link to the Creative Commons license, and indicate if changes were made.

References

- van Caneghem J, de Greef, J Block, C, Vandecasteele C (2015) *J Clean Prod* 112(5):4452–4460
- Peng Y, Li J, Si W, Luo J, Wang Y, Fu J, Li X, Crittenden J, Hao J (2015) *Appl Catal B* 168–169:195–202
- Kamata H, Takahashi K, Odenbrand CUI (1999) *J Mol Catal A* 139(2–3): 189–198
- Castellino F, Jensen AD, Johnsson JE, Fehrmann R (2009) *Appl Catal B* 86:196–205
- Castellino F, Jensen AD, Johnsson JE, Fehrmann R (2009) *Appl Catal B* 86:206–215
- Zheng Y, Jensen AD, Johnsson JE, Thørgersen JR (2008) *Appl Catal B* 83:186–194
- Odenbrand CUI, Lundin ST, Andersson L AH (1985) *Appl Catal* 18:335–352
- Odenbrand CUI, Andersson LAH, Brandin JGM, Lundin ST (1986) *Appl Catal* 27:363–377
- Khodayari R, Odenbrand CUI (1998) *Ind Eng Chem Res* 37(4):1196–1202
- Hanell B et al. (1996) *Värmeforsk*, ISSN 0282–3772, p 77
- Khodayari R, Odenbrand CUI (2001) *Appl Catal B* 33(4):277–291
- Magnusson M, Fridell E, Ingelsten H (2012) *Appl Catal B* 111–112: 20–26
- Barret EP, Joyner LG, Halenda PP (1951) *J Am Chem Soc* 73:373–380
- Odenbrand CUI, Brandin JGM to be published
- Lide D R (Ed.), (2008–2009) *Handbook of chemistry and Physics*, 89th edn. CRC Press, Boca Raton pp 4–99
- Mears DE (1971) *Ind Eng Chem Process Des Dev* 10(4):541–547
- Mears DE (1971) *J Catal* 20:127–131
- Mears DE (1976) *Ind Eng Chem Fundam* 15(1):20–23
- Baxter L, (2005) *Biomass impacts on SCR catalyst performance*, Technical report, IEA Bioenergy Task 32
- Guo X, Batholomew C, Hecker W and Baxter LL (2009) *Appl Catal B* 92: 30–40
- Satterfield CN (1991) *Heterogeneous catalysis in industrial practice*, 2nd edn. Mc Graw Hill, Inc., New York, pp 306–312
- Kamata H, Ohara H, Takahashi K, Yukimura A, Seo Y (2001) *Catal Lett* 73 (1):79–83
- Dunn TJ, Koppula TR, Stenger H, Wachs I (1998) *Appl Catal B* 19:103–117
- Lisi L, Lasorella G, Malloggi S, Russo G (2004) *Appl Catal B* 50:251–258
- Deng L, Liu X, Cao P, Zhao Y, Du Y, Wang C (2016) *J Energy Inst.* doi:10.1016/j.joei.2016.07.003
- Simonsen F (2006) *Analysteknik-Instrument och Metoder*, Studentlitteratur, Lund, Sweden, ISBN: 91-44-03613-2